

Statistical Emission of ${}^2\text{He}$ from Highly Excited Nuclear Systems

M. A. Bernstein and W. A. Friedman

Physics Department, University of Wisconsin, Madison, Wisconsin 53706

and

W. G. Lynch, C. B. Chitwood, D. J. Fields, C. K. Gelbke, and M. B. Tsang

National Superconducting Cyclotron Laboratory, Michigan State University, East Lansing, Michigan 48824

and

T. C. Awes, R. L. Ferguson, F. E. Obenshain, F. Plasil, R. L. Robinson, and G. R. Young

Oak Ridge National Laboratory, Oak Ridge Tennessee 37831

(Received 14 November 1984)

Correlations between two protons at small relative momenta are presented for ${}^{16}\text{O}$ -induced reactions on ${}^{12}\text{C}$ and ${}^{27}\text{Al}$ at 400 MeV. These data are well described by a statistical calculation which incorporates the thermal emission of the particle-unstable nucleus, ${}^2\text{He}$, from the compound nucleus. The good agreement suggests that the emission of particle-unstable light nuclei can be an important decay channel for highly excited nuclear systems, and can strongly influence two-particle correlations.

PACS numbers: 24.60.Dr, 21.40.+d, 23.90.+w, 25.70.Gh

As the excitation energy per nucleon is increased, new statistical mechanisms such as target fragmentation, or the statistical emission and subsequent decay of light particle-unstable nuclei (2n , ${}^2\text{He}$, ${}^2\text{H}^*$, α^* , ${}^5\text{He}$, ${}^5\text{Li}$, etc.), become important. While the emission of light particle-unstable nuclei has been safely neglected at low excitation energies, this process is expected to be important for the decay of highly excited nuclear systems ($T \gg 1$ MeV).¹⁻³ The positive identification of these decay channels requires the measurement of correlated fragments which are produced by the subsequent decay of the emitted particle-unstable nucleus.¹ In this Letter we test these concepts by comparing two-proton correlation data to calculations based on the statistical emission of ${}^2\text{He}$ from the compound nucleus and the subsequent decay of the two-proton virtual state.

In an experiment performed at the Holifield Heavy Ion Research Facility ${}^{12}\text{C}$ and ${}^{27}\text{Al}$ targets were bombarded with ${}^{16}\text{O}$ ions of 400-MeV incident energy. Light-particle correlations were measured with six ΔE - E telescopes which subtended individual solid angles of 0.76 msr and consisted of silicon ΔE and NaI E detectors. These telescopes were mounted in a close-packed hexagonal array which was centered at a scattering angle of 15° . The angular resolution and the angular separation between adjacent telescopes were 1.6° and 5.1° , respectively. Absolute cross sections, accurate to 10%, were obtained from the integrated beam current, the target thickness, and the solid angles of the telescopes. Energy calibrations, accurate to 3%, were obtained by measurement of the energies of recoil protons backscattered from a Mylar target by a 200-MeV ${}^{16}\text{O}$ beam.

A contour diagram for coincident protons produced

in reactions on the ${}^{12}\text{C}$ target at $\theta_{\text{lab}} = 15^\circ$ and relative proton angle of 5.1° is plotted in Fig. 1 as a function of the energies of the two protons. Because of limited statistics there is considerable uncertainty associated with the location of the contours. (Insufficient statistics precluded construction of a similar plot for the ${}^{27}\text{Al}$ target.) At nearly equal energies of the coincident protons, a situation which corresponds to small relative momenta, $\Delta p = |p_1 - p_2|/2 < 10$ MeV/c, there is a suppression of the cross section, while at slightly larger relative momenta, $\Delta p = 20$ MeV/c, broad maxima are observed for protons of 20–30 MeV. This dependence

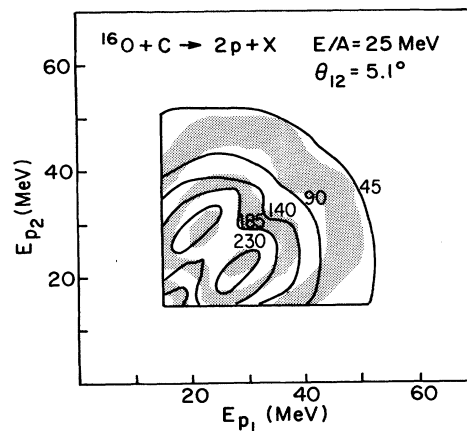


FIG. 1. Coincident cross sections. The solid lines indicate contours for the experimental cross section [$\mu\text{b}/(\text{MeV sr})^2$], produced in reactions on ${}^{12}\text{C}$ at $\theta_{\text{lab}} = 15^\circ$ and relative proton angle of 5.1° , as a function of the energies of the two protons. The alternating clear and shaded zones indicate the comparable contour regions calculated by the model described in the text.

on relative momentum is demonstrated more quantitatively by the correlation function $[1 + R(\Delta p)]$ defined by

$$\sigma(\mathbf{p}_1, \mathbf{p}_2) = C \sigma(\mathbf{p}_1) \sigma(\mathbf{p}_2) [1 + R(\Delta p)], \quad (1)$$

where $\sigma(\mathbf{p}_1, \mathbf{p}_2)$ and $\sigma(\mathbf{p}_i)$ denote the coincidence and the singles cross sections, respectively. The experimental correlation functions for the ^{12}C and ^{27}Al targets, shown in Fig. 2, were obtained by inserting the experimental cross sections in Eq. (1) and by summing both sides of the equation over all energies and angles corresponding to a given relative momentum. The normalization constant C has been determined by requiring that $R(\Delta p) = 0$ at $\Delta p = 70 \text{ MeV}/c$.

The light-particle inclusive spectra for ^{12}C and ^{27}Al , and the maxima in the coincidence cross section of Fig. 1, are compatible with considerable contributions from statistically emitting compoundlike residues⁴ (equilibrated residues from fusionlike reactions). For light targets these emitted particles are kinematically focused to forward angles in the laboratory. This stands in contrast to the negligible contributions at forward angles from compoundlike residues observed for ^{197}Au .⁴

We have calculated the correlations resulting from the statistical emission and subsequent decay of particle-unstable ^2He nuclei. For simplicity, emission from the fully equilibrated compound nucleus is as-

sumed. The spectra and multiplicities of ^2He and protons (as well as other nuclei in their particle-stable and unstable states) are calculated with the formalism of Ref. 5. This formalism approximates the distribution of individual decay chains by particle emission from one ensemble-averaged excited nucleus. The relative kinetic energy, E_r , of the two protons generated by ^2He decay is assumed to have the spectral distribution

$$\frac{dN(E_r)}{dE_r} \propto \exp\left(-\frac{E_r}{T}\right) \left(\frac{\exp(2\pi\eta) - 1}{\eta} \frac{\sin^2\delta}{E_r^{1/2}} \right). \quad (2)$$

The Boltzmann factor incorporates the phase-space constraints imposed by the compound nucleus which is at temperature T . The second factor arises from the Watson-Migdal approximation.^{6,7} It contains information pertaining to the Coulomb repulsion through the Sommerfeld parameter η , and the singlet s virtual state through the phase shift δ . The Boltzmann factor also serves to cut off the high-relative-energy contributions for which the Watson-Migdal expression is invalid. The ^2He spectrum is combined with Eq. (2) to obtain the proton spectra in the laboratory frame of reference.

In addition to protons from the decay of the ^2He , we include coincident protons which are emitted sequentially from the compound nucleus. For light targets, the coincidence cross section for sequentially evaporated protons is sensitive to constraints imposed by momentum conservation.⁸ To take these effects into account, we require that the residual nucleus recoils coherently from the emission of the first proton and that the second proton is emitted from this recoiling system. For simplicity, it is assumed that the more energetic proton is emitted first, and that the recoiling system is the ensemble-averaged compound nucleus at the average temperature for proton emission. For low-energy protons, the recoil corrections have a small effect; however, the importance of momentum conservation increases with the energy of the detected proton. The mean separation between sequentially evaporated protons, corresponding to the parameter $v\tau$ in Koonin's model,⁹ is rather large (25–30 fm). For this reason we neglect final-state interactions between independently emitted protons. We estimate that the greatest corrections to the correlation caused by final-state interactions between these sequentially evaporated protons should occur at small relative momenta ($\Delta p < 15 \text{ MeV}/c$) where the long-ranged Coulomb interaction is dominant. In calculating the correlation cross section we have also neglected contributions from noncompound emission of protons. This is consistent with the magnitudes of the fusion cross sections which are assumed. The magnitude of noncompound contributions cannot easily be determined experimentally, since for light targets, the compound

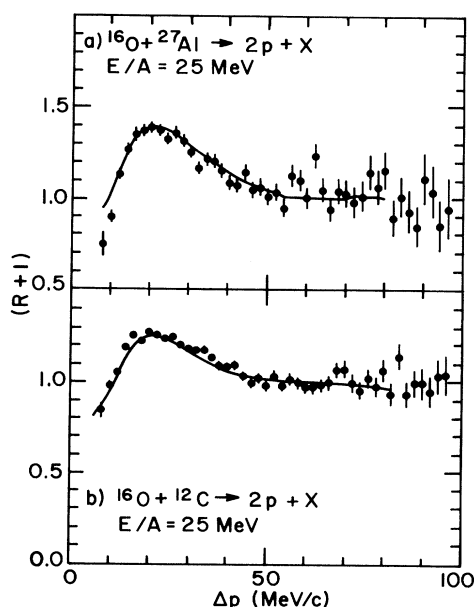


FIG. 2. (a) The experimental correlation function $1 + R(\Delta p)$ plotted as a function of the relative momentum for protons produced in reactions on the ^{27}Al target. The theoretical correlation function is drawn as the solid line. (b) Corresponding experimental and theoretical correlation functions for reactions on the ^{12}C target.

and noncompound emissions are not kinematically separated.

The spectra and multiplicities for ${}^2\text{He}$ and protons were calculated with the formalism of Ref. 5. This formalism predicts the multiplicities to be respectively 0.16 and 2.4 for the ${}^{12}\text{C}$ target, and 0.22 and 2.9 for the ${}^{27}\text{Al}$ target. Initial temperatures, 9.4 MeV for mass 28 (${}^{12}\text{C}$ target) and 9.9 MeV for mass 43 (${}^{27}\text{Al}$ target), follow from the assumption of a completely fused system treated as a Fermi gas with Fermi energies of 25 and 33 MeV for the mass-28 and -43 systems. These energies are consistent with information from electron scattering.¹⁰

The calculated coincidence cross section for the ${}^{12}\text{C}$ target is shown in Fig. 1. This calculation was performed with use of the exact experimental detector configuration as input. It was determined to be insensitive to angular-averaging effects arising from the finite detector solid angles. The calculated correlation is in excellent agreement with the data. A fusion cross section of 475 mb is required to match the peak of the experimental coincidence cross section of $250 \mu\text{b}/(\text{MeV sr})^2$ which occurs at E_1 and E_2 equal to 21 and 28 MeV, respectively. This corresponds to about 45% of the geometric cross section. The theoretical correlation functions $1 + R(\Delta p)$ for the ${}^{12}\text{C}$ and ${}^{27}\text{Al}$ targets, normalized to 1 at 70 MeV/c (as were the data), are drawn as solid lines in Fig. 2. It should be noted that the correlation function in Fig. 2 is insensitive to the fusion cross section, and therefore the excellent agreement is obtained here without any adjustable parameters.

Further information may be gained by investigation of the correlation function $1 + R(\Delta p)$ as a function of the total energy of the two coincident protons. This energy dependence for reactions on the ${}^{12}\text{C}$ and ${}^{27}\text{Al}$ targets is shown in Fig. 3 for the relative momentum intervals of $\Delta_1 p = 15\text{--}25 \text{ MeV}/c$ (where the singlet s state strongly contributes) and $\Delta_2 p = 50\text{--}70 \text{ MeV}/c$ (where the calculated correlation function primarily reflects contributions from noninteracting sequentially emitted protons). The decrease of the correlation functions with total proton energy for the large-relative-momentum bin $\Delta_2 p$ arises from the influence of momentum conservation on the correlation between sequentially emitted protons.¹¹ The structure in the calculated correlation functions for the small-relative-momentum bin $\Delta_1 p$ depends in a detailed way on the differences between the spectra for ${}^2\text{He}$ and for protons, and also on the Jacobians arising from kinematic coordinate-frame transformations.

The correlation functions reported earlier¹¹ in ${}^{16}\text{O}$ reactions on ${}^{197}\text{Au}$ are considerably larger at $\Delta p = 20 \text{ MeV}/c$ than those shown here. The emission of ${}^2\text{He}$ from equilibrated compound nuclei cannot account for the correlations observed with the ${}^{197}\text{Au}$ target. In

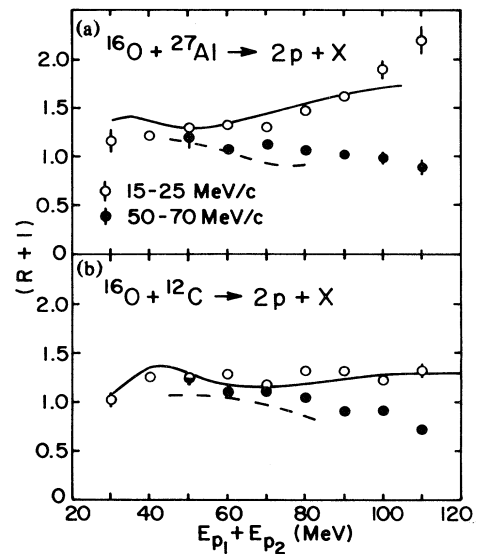


FIG. 3. (a) The correlation function $1 + R(\Delta p)$, gated on relative momentum intervals of 15–25 and 50–70 MeV/c, plotted as a function of the sum energy of the two protons for reactions on the ${}^{27}\text{Al}$ target. The theoretical correlation functions at the two momentum intervals are drawn as solid and dashed lines. (b) Corresponding experimental and theoretical correlation functions for reactions on the ${}^{12}\text{C}$ target.

particular for correlations measured at forward angles with heavy targets, e.g., Ref. 11, the contributions from compound-nuclear emission are negligible⁴ compared to those from other processes such as direct or preequilibrium emission. In addition, the calculated multiplicity of ${}^2\text{He}$ statistically emitted from compound nuclei formed in reactions with the ${}^{197}\text{Au}$ target is smaller by a factor of 10 than multiplicities calculated for ${}^{12}\text{C}$ and ${}^{27}\text{Al}$ targets, while the proton inclusive cross sections are comparable.

In summary, for ${}^{16}\text{O}$ -induced reactions on ${}^{12}\text{C}$ and ${}^{27}\text{Al}$ targets, correlations between emitted protons have been observed which are consistent with energy and angular distributions resulting from the statistical emission of the particle-unstable nucleus ${}^2\text{He}$ from the compound nucleus. This suggests the relevance of this process for highly excited nuclear systems. While the cases considered in this Letter involve emitting systems (compound nuclei) which exhibit properties of global equilibrium, a similar mechanism involving ${}^2\text{He}$ emission can be important for systems assumed to have small regions of local equilibrium. Such a mechanism could offer an alternative interpretation to observations previously discussed in terms of the non-statistical model of Koonin.⁹ Systematic studies of other light-particle correlations (e.g., p - d , p - t , etc., correlations) can help determine the relative importance of the statistical and nonstatistical contributions

to those cases.

This work was supported in part by the National Science Foundation under Grants No. PHY 83-12245 and No. PHY 82-04302 and the U. S. Department of Energy under Contract No. DE-AC05-84OR21400 with Martin Marietta Energy Systems.

¹M. A. Bernstein *et al.*, Phys. Rev. C **29**, 132 (1984), and **30**, 412(E) (1984).

²J. Gosset *et al.*, Phys. Rev. C **18**, 844 (1978).

³H. Stocker, J. Phys. G. **10**, L111 (1984).

⁴M. B. Tsang *et al.*, to be published.

⁵W. A. Friedman and W. G. Lynch, Phys. Rev. C **28**, 16 (1983).

⁶K. M. Watson, Phys. Rev. **88**, 1163 (1952).

⁷A. B. Migdal, Zh. Eksp. Teor. Fiz. **28**, 3 (1955) [Sov. Phys. JETP **1**, 2 (1955)].

⁸W. G. Lynch *et al.*, Phys. Lett. **108B**, 274 (1982).

⁹S. E. Koonin, Phys. Lett. **70B**, 43 (1977).

¹⁰E. J. Moniz *et al.*, Phys. Rev. Lett. **26**, 445 (1971).

¹¹W. G. Lynch *et al.*, Phys. Rev. Lett. **51**, 1850 (1983).